ANNALS OF WEST UNIVERSITY OF
TIMISOARA PHYSICS
Vol. LXVII, 2025

DOI: 10.2478/awutp-2025-0008

ALTITUDE ADJUSTMENT OF EMPIRICAL MODELS FOR ESTIMATING CLEAR-SKY SOLAR IRRADIANCE

Anamaria-Giulia Goilean, Eugenia Paulescu, Marius Paulescu*

Faculty of Physics, West University of Timisoara, V Parvan 4, 300223, Timisoara, Romania
**Corresponding author: marius.paulescu@e-uvt.ro*

Article Info

Received: 04.10.2025
Accepted: 27.10.2025

Keywords:
Solar irradiance; empirical model; geographical altitude; linear regression.

Abstract

This research provides an innovative empirical model for solar irradiance estimation under clear sky conditions. The new model adjusts the estimates of G-EM clear-sky solar irradiance model (Goilean et al. AWUT-Physics 66, 2024, 241) with respect to site altitude. The study was conducted based on a synthetically obtained dataset, generated using two high-performance clear-sky solar irradiance parametric models. Preliminary tests were performed against high quality clear-sky radiometric data. The results demonstrate that explicit insertion of altitude as an input parameter of G-EM enhances their performance in mountain locations, thus expanding its geographical area of applicability.

1. Introduction

The clear-sky solar irradiance models can be roughly classified into three categories based on the input parameters: empirical, parametric and spectral models [1]. This study focuses on the first category, namely empirical models. The class of empirical models comprises the simplest clear sky solar irradiance models fitted on data acquired over a specific geographical area. The close connection of an empirical model with its native location is given by the inclusion of the local atmospheric transmittance in the fitted coefficients. Empirical models depend only on deterministic input parameters, namely zenith angle, local altitude, and Julian day. In contrast to empirical solar irradiance models, spectral/parametric models, estimate the atmospheric transmittance considering some measured atmospheric parameters, such as ozone column content, water vapor column content, aerosol properties, as input parameters.

Empirical clear sky solar irradiance models are briefly introduced next. Many empirical models were developed starting with the 1970s. The Hottel model [2] uses the Sun's elevation angle and site altitude as input parameters. It can be applied up to altitudes of 6 km and estimates direct-normal solar irradiance. The Bugler model [3] uses only the Sun's elevation angle as an input parameter. It estimates diffuse solar irradiance. The Bugler model can be effectively used together with the Hottel model to calculate global solar irradiance. The Adnot et al. model [4] also uses the Sun's elevation angle as an input parameter and estimates clear sky global solar irradiance. The Adnot et al. model proved to be very efficient in the Romanian climate after tests against radiometric data collected from Timisoara, Constanta and Craiova [5]. The EIM model [5] calculates global solar irradiance as a function of the Sun's elevation angle, too. The model is built using data recorded under clear sky conditions at the meteorological station of Timisoara, Romania.

The exhaustive report [6] compares the performance of 95 models for direct and diffuse clear-sky solar irradiance, including empirical models. The results highlight the empirical model of Biga [7]. Despite requiring only deterministic input data, it achieved the 10th position in the ranking for estimating diffuse solar irradiance in harsh cold environments. This argues for the practical importance of empirical models in modeling solar irradiance.

The aim of the study is to develop a methodology for expanding the area of applicability of clear sky solar irradiance models targeting to enhance their accuracy in mountainous locations. The proposed methodology is presented as a case study, showing the incorporation of altitude into G-EM [8], a clear-sky solar irradiance model developed by us. G-EM [8] was derived based on experimental data obtained on the Solar Platform of the West University of Timisoara [9]:

$$G_a(\theta_z, j) = G_{SC} \varepsilon_j a (cos\, \theta_z)^{b-1} cos\, \theta_z \quad (1)$$

The G-EM equation employs atmospheric optical mass (via the Sun zenith angle θ_z) and Julian day j, as input parameters. G_{SC} = 1361.1 W/m^2 represents the solar constant while ε_j denotes the correction of G_{SC} in accordance with the Earth's orbit eccentricity. Formally, this is a Long and Ackerman -type equation [10], calibrated for the Pannonian Plain.

The rest of the paper is organized as follows: the new model is introduced in the next section, along with a detailed presentation of the methodology. Section 3 presents results of testing the new model against data collected at radiometric stations around the world. Section 4 summarizes the main conclusions.

2. New empirical model

2.1 Synthetic data

To develop the new model, synthetic clear-sky global solar irradiance data series were generated for altitudes between 0 and 5 km with a sampling of 0.25 km. For each altitude, the zenith angle was varied between 0 to 90 degrees. Two different parametric models, REST2 [11] and PEM [12] were chosen to generate the data series. REST2 is a parametric model which estimates solar irradiance under clear sky conditions with high accuracy, being considered one of the most performant models in the world. PEM is a parametric model developed by us, demonstrating performance comparable with REST2 [12]. The models differ in their structure and differently account for the specific atmospheric transmittances. The two models were run with average values of atmospheric parameters, corresponding to clear sky conditions in temperate regions. These input parameters are ozone column content $l_{O3} = 0.35$ cm, water vapor column content $\mathrm{w} = 1.42$ cm, the Ångström exponent $\alpha = 1.3$ and the Ångström turbidity coefficient $\beta = 0.07$.

2.2. Model development

In the first step, the G-EM equation was fitted to the data sets generated at various altitudes. Table 1 shows the results of fitting the G-EM equation at quantified altitude intervals. The results are expressed as the coefficients a and b, subsequently used to obtain a new empirical equation, which includes altitude as input. Figure 1 shows that the coefficients a and b exhibit a linear variation with altitude z. This linear variation leads to the equation of the new empirical model:

$$G_z(\theta_z, j, z) = G_{SC}\varepsilon_j(c + dz)(\cos\theta_z)^{f-1+gz}\cos\theta_z \qquad (2)$$

The linear association between the fitted coefficients and altitude is expressed by the parameters c, f, intercept parameters, and d, g, the slope parameters. The applicability of linear models to capture the altitude dependence of the coefficients is given by the close correspondence between the linear curves and generated data. Practically, at the second step of building the G_z model, the empirical coefficients c, d, f and g from Eq. (2) were fitted (Fig. 1).

The values of these coefficients depend on the source model. Thus, the following two sets of coefficients were obtained: $c = 0.8176$, $d = 0.0047$, $f = 1.2083$, $g = -0.006$ with data generated by REST2 and $c = 0.8059$, $d = 0.0028$, $f = 1.2329$, $g = -0.0044$ with data generated by PEM.

Table 1. The fitted coefficients a and b of the G-EM equation (Eq. 1) at different altitudes z

z [km]	*a*	*b*	*z* [km]	*a*	*b*
0	0.8061	1.2324	2.75	0.8137	1.2210
0.25	0.8067	1.2314	3	0.8144	1.2199
0.5	0.8074	1.2304	3.25	0.8151	1.2187
0.75	0.8081	1.2294	3.5	0.8158	1.2176
1	0.8088	1.2284	3.75	0.8166	1.2164
1.25	0.8095	1.2274	4	0.8173	1.2152
1.5	0.8101	1.2264	4.25	0.8181	1.2140
1.75	0.8108	1.2250	4.5	0.8188	1.2127
2	0.8115	1.2243	4.75	0.8196	1.2114
2.25	0.8122	1.2232	5	0.8203	1.2101
2.5	0.8129	1.2221			

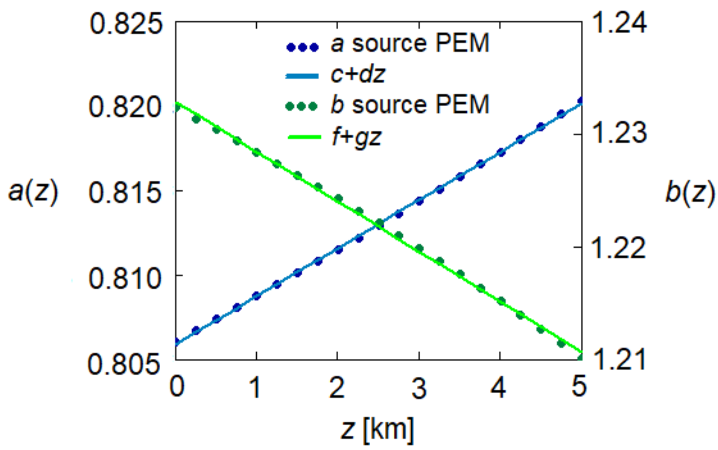

Figure 1. Altitude-related variability of coefficients *a* and *b* (Eq. 1) fitted on PEM-derived synthetic irradiance data. Linear regression approximations for *a* and *b* are displayed.

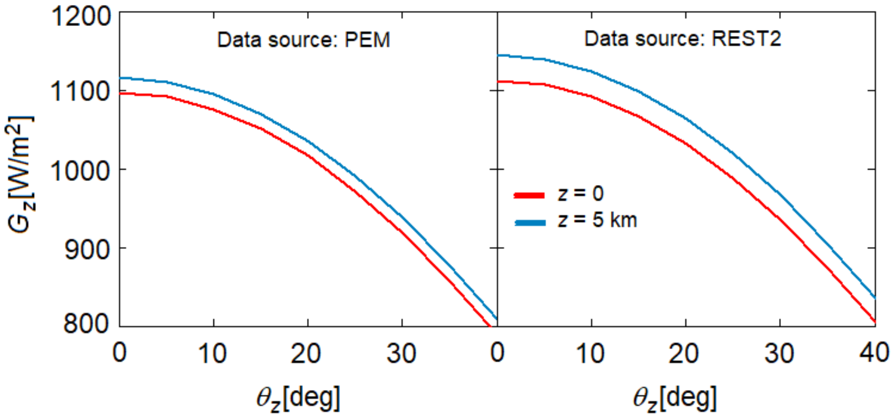

Figure 2. Estimated global solar irradiance G_z at ground level (z = 0) and at the highest altitude (z = 5 km). G_z was built on synthetic data generated by two parametric clear-sky solar irradiance models REST2 [11] and PEM [12]

The estimated value G_z is conditioned by the source model implemented for generating synthetic data (Fig. 2). Each parametric model has a particular way of integrating altitude, which result in a different impact on the estimated global solar irradiance. The PEM and REST2 models show differences in the way they simulate global solar irradiance at different altitudes. As can be seen in Fig.2, the REST2 model estimates higher values of solar irradiance compared to the PEM model. Figure 2 also shows that the difference between the curve corresponding to ground level (z = 0) and the one corresponding to the highest altitude (z = 5 km) is wider using REST2 than using PEM. Based on these results, it is not possible to determine which of the two G_z variants, based on REST2 and PEM, is more efficient. To correctly evaluate the performance of G_z, a comparison of the estimates with measured data is necessary. What can be concluded after this analysis is that the different source models significantly influence the values of the fitted empirical parameters.

Finally, it is worth mentioning that the new model G_z is inspired by the physics of solar radiation transfer in the atmosphere. Let's prove this statement. Global solar irradiance is estimated by a parametric model based on the following generic equation:

$$G(\theta_z, j, l_{O_3}, l_w, z, \beta, \alpha) = G_{sc}\varepsilon_j \overline{\tau_{atm}} \cos\theta_z \tag{3}$$

where $\overline{\tau_{atm}}$ denotes the atmospheric transmittance:

$$\overline{\tau_{atm}} = \bar{\tau}_{O_3}(\theta_z, l_{O_3})\bar{\tau}_w(\theta_z, l_w)\bar{\tau}_g(\theta_z)\big(1 + \bar{\tau}_R(\theta_z, z)\bar{\tau}_a(\theta_z, \beta, \alpha)\big) \tag{4}$$

The terms $\bar{\tau}_g(\theta_z)$, $\bar{\tau}_{O_3}(\theta_z, l_{O_3})$, $\bar{\tau}_w(\theta_z, l_w)$, $\bar{\tau}_a(\theta_z, \beta, \alpha)$ and $\bar{\tau}_R(\theta_z, z)$ represent the specific atmospheric transmittances (see e.g. [5]) and model trace gases absorption, ozone absorption, water vapor absorption, aerosols scattering and Rayleigh scattering, respectively.

Equation (2) represents a formally equivalent form of Eq. (3). By analyzing the equations, it results that the atmospheric transmittance in the proposed model is determined by:

$$\overline{\tau_{atm}} = (c + dz)(cos\,\theta_z)^{f-1+gz} \quad (5)$$

The atmospheric transmittance at a given zenith angle is encapsulated into the fitted coefficients.

3. Model testing

3.1. Test data

The empirical G_z model was validated using radiometric data recorded at 12 BSRN radiometric stations, globally distributed (Figure 3). Baseline Surface Radiometric Network, BSRN, is an observational network initiated under the World Climate Research Program (WCRP) to provide high-precision measurements of surface solar radiation. BSRN data are fundamental for evaluating and refining climate models, as even small fluctuations in surface irradiance can notably influence climate systems [13].

The BSRN stations were chosen from different climatic zones. Two stations experience a Mediterranean climate: the Carpentras station (BSRN index: CAR), located at an altitude of 100 m, in France, and the Izana station (BSRN index: IZA), located at 2,372 m altitude, in Spain. The Cener station (BSRN index: CNR), located at an altitude of 471 m, in Spain, experiences a temperate climate. The Darwin station (BSRN index: DAR), located at an altitude of 30 m, in Australia, experiences a tropical savanna climate. The Fukuoka station (BSRN index: FUA), located at an altitude of 3 m, in Japan, experiences a humid subtropical climate. The Hampton station (BSRN index: LRC), located at 3 m altitude, in the United States, comparable to Fukuoka, experiences a humid subtropical climate. Xianghe station (BSRN index:XIA), located at 32 m altitude, in China, was also selected for the subtropical climate. The Gobabeb station (BSRN index: GOB), located at an altitude of 407 m, in Namibia, experiences a semi-arid climate. The Palaiseau station (BSRN index: PAL), located at 156 m altitude, in France, experiences a temperate oceanic climate. Two stations were selected for the desert climate: Sede Boqer (BSRN index: SBO), located at 500 m altitude, in Israel and

Tamanrasset (BSRN index: TAM), located at 1,385 m altitude, in Algeria. The Toravere station (BSRN index: TOR), located at 70 m altitude, in Estonia, is selected for the continental climate.

Figure 3. Points on the world map indicating the BSRN station from where the test data were collected

3.2. Testing results

Figure 4 summarizes the relationship between measured global irradiance G_m and estimated global irradiance G_e using data from 5 representative stations with different altitudes and climatic conditions (CAR, CNR, GOB, TAM, IZA) as well as for all stations together. Visual inspection shows that the insertion of altitude into G-EM equation determines a higher accuracy in the estimating global solar irradiance. The strongest correspondence between the measured and estimated global irradiance is obtained for the CAR (alt. 0.1 km) and CNR (alt. 0.471 km) stations, both having temperate mediterranean climates being sited at mid-range altitudes. As expected, (due to the atmospheric conditions assumed in the fitting process), G_z is more efficient at low to moderate altitudes, experiencing average temperate conditions. A significant deviation can be observed in the case of the TAM and IZA station, both located at high altitude highlighting the difficulty of modeling solar irradiance under limiting conditions. In contrast to the high performance corresponding to the CAR station, the IZA station, with a mediterranean climate and located at a high altitude (2.372 km), shows discrepancies between measured and estimated data. Compared with the performance at the TAM station, the GOB station, positioned at a lower altitude (0.407 km) and experiencing a semi-arid climate like Tamanrasset, provides a better estimate. It can thus be seen that the accuracy of the model is determined by both local altitude and climate. The closer the climate is to that of origin, the better performance can be expected.

Overall results show that considering altitude in the estimation increases the model performance. Also, the choice of source (REST2 vs. PEM) and model type (G_z vs. G-EM) has an impact on the accuracy, as reflected by the dispersion and non-uniform alignment of the data points in Fig.4.

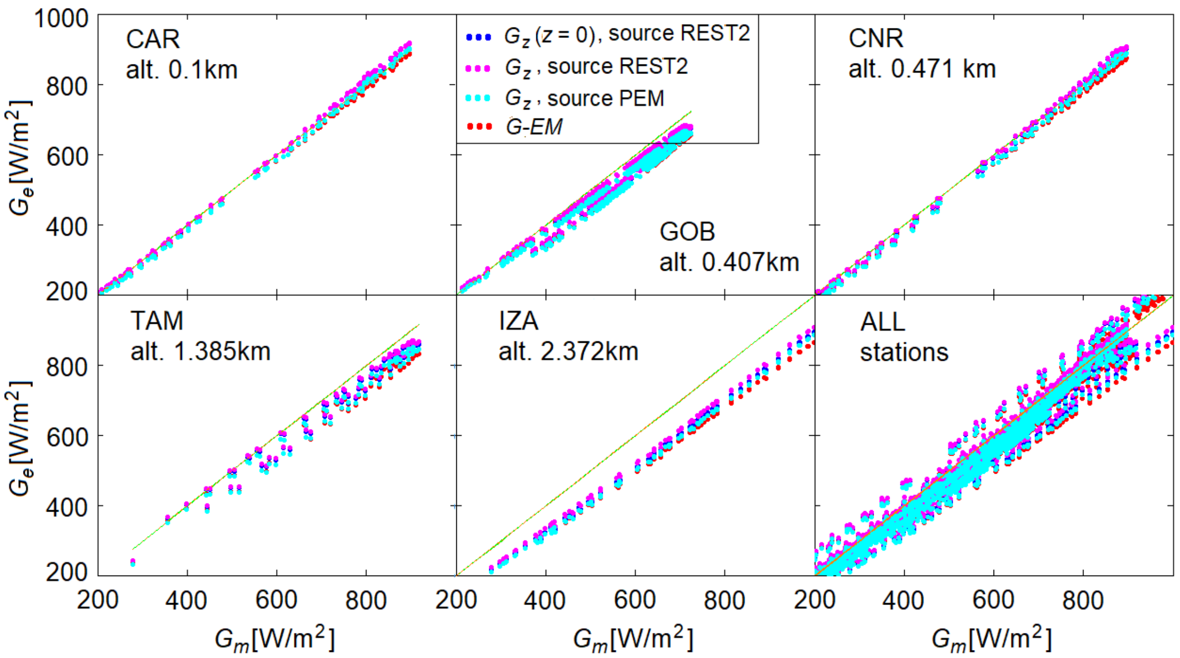

Figure 4. Estimated G_e versus measured G_m global solar irradiance at five selected stations. Each frame corresponds to a station. The green line indicates the first diagonal

Table 2. Statistical indicators of the accuracy of global solar irradiance estimation using the empirical models G-EM (Eq. 1) and G_z (Eq. 2), with REST2 as source.

Station	Altitude [km]	G-EM		G_z	
		nRMSE	*nMBE*	*nRMSE*	*nMBE*
FUA	0.003	0.028	-0.022	0.028	-0.022
LRC	0.003	0.103	-0.094	0.103	-0.094
DAR	0.03	0.026	0.023	0.027	0.023
XIA	0.032	0.019	-0.011	0.19	-0.011
TOR	0.07	0.030	-0.028	0.29	-0.025
CAR	0.1	0.023	0.015	0.023	0.016
PAL	0.156	0.049	-0.039	0.048	-0.038
GOB	0.407	0.062	-0.054	0.059	-0.050
CNR	0.471	0.020	-0.001	0.020	0.002
SBO	0.5	0.104	0.104	0.109	0.108
TAM	1.38	0.059	-0.050	0.050	-0.040
IZA	2.37	0.144	-0.141	0.125	-0.122
ALL		0.066	-0.026	0.063	-0.022

Table 2 summarizes the values of the statistical indicators (nRMSE and nMBE, defined in Appendix A) applied for the comparison of the G-EM performance with the one of the new altitude-dependent model G_z It can be seen that the statistical indicators for the altitude-dependent model G_z differ from those corresponding to the G-EM model in the case of stations positioned at high altitude, as is the case for TAM (1.38 km) and IZA (2.37 km). It is thus highlighted that the atmospheric effect on solar irradiance in high altitude regions can be captured by including altitude in the model.

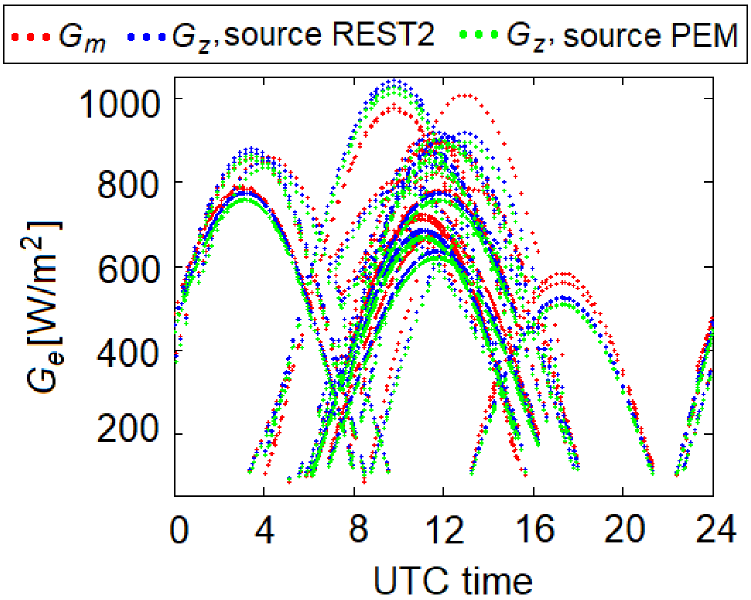

Figure 5. Illustration of measured and estimated global solar irradiance plotted with respect to time. All data from the test dataset are considered

Figure 5 shows the relative contribution of the REST2 and PEM-based parametric models to the estimates provided by the empirical G_z model. The presence of smooth, bell-shaped curves, in all data sequences is specific to clear-sky conditions and demonstrates that the measurements were made on clear days. The differences in longitudinal positioning between the radiometric stations explain the temporal shifts of the irradiance maxima, which is due to the occurrence of solar noon at different UTC times. It is noted that the empirical model built using REST2 (blue curve), as well as the one using PEM (green curve), follows the global trend of the measured irradiance values with satisfactory accuracy. This alignment of the results shows that the empirical models can function as credible means of estimating solar irradiance under clear-sky conditions, even without the support of atmospheric input parameters.

4. Conclusions

The applicability domain of the empirical clear sky solar irradiance model G-EM [8] was broadened by incorporating altitude as a model parameter. An original method was developed for building the new model. The new method is based on synthetic data generated with a parametric model. Tests performed against a challenging set of radiometric data, collected from stations spread around the world, show that including altitude in the list of input parameters improves the accuracy of estimates for mountainous locations. Overall, the results confirm the efficiency of empirical models obtained from the use of synthetically generated data. Since pure empirical models allow only deterministic input variables, the dominant uncertainty in the estimation of global solar irradiance is induced by the state of the atmosphere. Deviations of atmospheric parameters from the values to which an empirical model has been fitted can produce errors much larger than those determined by the lack of altitude in the model. The case study in the paper provides the equation and model parameters for temperate regions. In principle, a user can set model parameters for any climate of interest, just by following the proposed methodology.

Appendix

A. Statistical indicators of accuracy

Two of the most commonly used statistical indicators for assessing accuracy in modeling are the mean bias error (MBE) and the root mean square error (RMSE):

$$MBE = \frac{1}{N}\sum_{i=1}^{N}(c_i - m_i) \quad \text{(A1)}$$

$$RMSE = \left[\frac{1}{N}\sum_{i=1}^{N}\left(c_i - m_i\right)^2\right]^{1/2} \quad \text{(A2)}$$

where c and m denote the estimated and measured quantities, respectively. While MBE is associated with a measure of systematic errors (or bias), RMSE is a measure of random errors. To ensure comparability of model performance across samples of different magnitudes, the indicators are normalized to the mean of the experimental data ($\mu = \frac{1}{N}\sum_{i=1}^{N} m_i$) :

$$nMBE = MBE/\mu \quad \text{(A3)}$$

$$nRMSE = RMSE/\mu \quad \text{(A4)}$$

References

[1] Paulescu E, Paulescu M, Hategan S, *Integration of spectral atmospheric transmittances. Parametric models for solar irradiance*. In Spectral Characteristics of Solar Radiation, Applications in Photovoltaic Conversion, Elsevier (2025).

[2] Hottel HC, *A simple model for estimating the transmittance of direct solar radiation through clear atmosphere*, Solar Energy 18, (1976), 129 – 139.

[3] Bugler JW, *The determination of hourly insolation on an inclinated plane using a diffuse irradiance model based on hourly measured global horizontal insolation*, Solar Energy 19, (1977), 4 – 11.

[4] Adnot J, Bourges B, Campana D, Gicquel R (1979) *Utilisation des courbes de frequence cumulees pour le calcul des installation solaires.* In Analise Statistique des Processus Meteorologiques Appliquee a l'Energie Solaire, Lestienne R. Paris, pp.9-40, (1979).

[5] Paulescu M, Schlett Z, *A simplified but accurate spectral solar irradiance model*, Theoretical and Applied Climatology 2003, 75, 203-212.

[6] Sun X, Bright JM, Gueymard CA, Bai X, Acord B, Wang P, *Worldwide performance assessment of 95 direct and diffuse clear-sky irradiance models using principal component analysis*, Renewable and Sustainable Energy Reviews 135, (2021), 110087.

[7] Biga A.J, Rosa Rui, *Contribution to the study of the solar radiation climate of Lisbon*, Solar Energy 23(1), (1979), 61–67.

[8] Goilean AG, Paulescu E, Paulescu M, *A Physically Inspired Model for Estimating Clear-Sky Solar Irradiance*, Annals of West University of Timisoara - Physics 66, (2024), 241-250.

[9] Solar Platform of the West University of Timisoara. http://solar.physics.uvt.ro/srms/ (Accessed August 2025)

[10] Long CN, Ackerman TP, *Identification of clear skies from broadband pyranometer measurements and calculation of downwelling shortwave cloud effects.* Journal of Geophysical Research 105(D12), (2000), 15609–15626.

[11] Gueymard CA. REST2: *High-Performance solar radiation model for cloudless-sky irradiance, illuminance, and photosynthetically active radiation – validation with a benchmark dataset,* Solar Energy 82, (2008), 272–285.

[12] Paulescu E, Paulescu M, *A new clear sky solar irradiance model*, Renewable Energy 179 (2021) 2094–2103.

[13] Baseline Surface Radiation Network. https://bsrn.awi.de/ (Accessed August 2025).